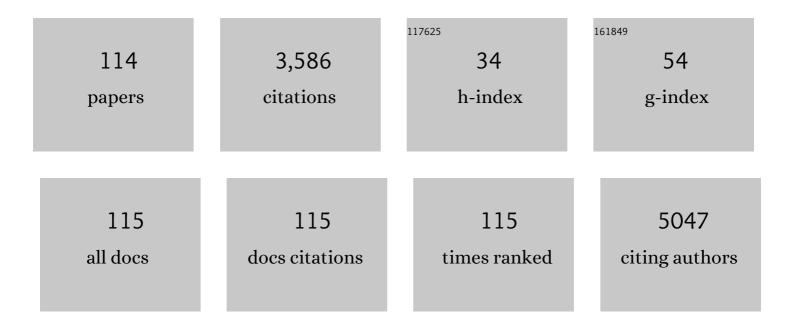
Sayan Bhattacharyya

List of Publications by Year in descending order

Source: https://exaly.com/author-pdf/1473275/publications.pdf Version: 2024-02-01



#	Article	IF	CITATIONS
1	Cs ₃ Bi ₂ I ₉ nanodiscs with phase and Bi(<scp>iii</scp>) state stability under reductive potential or illumination for H ₂ generation from diluted aqueous HI. Nanoscale, 2022, 14, 4281-4291.	5.6	9
2	Pressure-induced emission enhancement and bandgap narrowing: Experimental investigations and first-principles theoretical simulations on the model halide perovskite <mml:math xmlns:mml="http://www.w3.org/1998/Math/MathML"><mml:msub><mml:mrow><mml:mi>Cs</mml:mi>Physical Review B, 2022, 105, .</mml:mrow></mml:msub></mml:math>	nrðŵ> <mr< td=""><td>nl:mn>3</td></mr<>	nl:mn>3
3	The Perfect Imperfections in Electrocatalysts. Chemical Record, 2022, 22, .	5.8	9
4	Thickness-Attuned CsPbBr ₃ Nanosheets with Enhanced <i>p</i> -Type Field Effect Mobility. Journal of Physical Chemistry Letters, 2021, 12, 1560-1566.	4.6	17
5	Pressure-Induced Emergence of Visible Luminescence in Lead Free Halide Perovskite Cs ₃ Bi ₂ Br ₉ : Effect of Structural Distortion. Journal of Physical Chemistry C, 2021, 125, 3432-3440.	3.1	12
6	In Situ Cation Intercalation in the Interlayer of Tungsten Sulfide with Overlaying Layered Double Hydroxide in a 2D Heterostructure for Facile Electrochemical Redox Activity. Inorganic Chemistry, 2021, 60, 6911-6921.	4.0	17
7	Heterovalent Substitution in Mixed Halide Perovskite Quantum Dots for Improved and Stable Photovoltaic Performance. Journal of Physical Chemistry C, 2021, 125, 5485-5493.	3.1	18
8	Unraveling the Charge Transport Mechanism in Mechanochemically Processed Hybrid Perovskite Solar Cell. Langmuir, 2021, 37, 5513-5521.	3.5	11
9	Photodetectors with High Responsivity by Thickness Tunable Mixed Halide Perovskite Nanosheets. ACS Applied Materials & Interfaces, 2021, 13, 43104-43114.	8.0	19
10	Comprehensive and Highâ€ŧhroughput Electrolysis of Water and Urea by 3–5â€nm Nickel and Copper Coordination Polymers. Chemistry - an Asian Journal, 2021, 16, 3444-3452.	3.3	7
11	An unconventional route to an ambipolar azaheterocycle and its <i>in situ</i> generated radical anion. Organic and Biomolecular Chemistry, 2021, 19, 5114-5120.	2.8	4
12	Bimetallic Zero-Valent Alloy with Measured High-Valent Surface States to Reinforce the Bifunctional Activity in Rechargeable Zinc-Air Batteries. ACS Sustainable Chemistry and Engineering, 2021, 9, 14868-14880.	6.7	9
13	Core/Shell Nanocrystal Tailored Carrier Dynamics in Hysteresisless Perovskite Solar Cells with â^1⁄420% Efficiency and Long Operational Stability. Journal of Physical Chemistry Letters, 2020, 11, 591-600.	4.6	21
14	Charge Transport between Coaxial Polymer Nanorods and Grafted All-Inorganic Perovskite Nanocrystals for Hybrid Organic Solar Cells with Enhanced Photoconversion Efficiency. Journal of Physical Chemistry C, 2020, 124, 246-255.	3.1	11
15	Tweaking Nickel with Minimal Silver in a Heterogeneous Alloy of Decahedral Geometry to Deliver Platinumâ€like Hydrogen Evolution Activity. Angewandte Chemie, 2020, 132, 2903-2911.	2.0	6
16	Tweaking Nickel with Minimal Silver in a Heterogeneous Alloy of Decahedral Geometry to Deliver Platinumâ€like Hydrogen Evolution Activity. Angewandte Chemie - International Edition, 2020, 59, 2881-2889.	13.8	50
17	Spin Disorder and Particle Size Effects in Cobalt Ferrite Nanoparticles with Unidirectional Anisotropy and Permanent Magnet-like Characteristics. Journal of Physical Chemistry C, 2020, 124, 25992-26000.	3.1	13

Shaping a Doped Perovskite Oxide with Measured Grain Boundary Defects to Catalyze Bifunctional18Oxygen Activation for a Rechargeable Znâ€"Air Battery. ACS Applied Materials & amp; Interfaces, 2020, 12, 8.0 2340355-40363.

#	Article	IF	CITATIONS
19	An electrochemically reversible lattice with redox active A-sites of double perovskite oxide nanosheets to reinforce oxygen electrocatalysis. Chemical Science, 2020, 11, 10180-10189.	7.4	14
20	Hot Phonon and Auger Heating Mediated Slow Intraband Carrier Relaxation in Mixed Halide Perovskite. IEEE Journal of Quantum Electronics, 2020, , 1-1.	1.9	1
21	2D Heterojunction Between Double Perovskite Oxide Nanosheet and Layered Double Hydroxide to Promote Rechargeable Zincâ€Air Battery Performance. ChemElectroChem, 2020, 7, 5005-5012.	3.4	19
22	Oxygenâ€Defectâ€Rich Cobalt Ferrite Nanoparticles for Practical Water Electrolysis with High Activity and Durability. ChemSusChem, 2020, 13, 3875-3886.	6.8	52
23	Thermal Nonlinear Refraction in Cesium Lead Halide Perovskite Nanostructure Colloids. Journal of Physical Chemistry C, 2020, 124, 15558-15564.	3.1	5
24	Charge transfer from perovskite oxide nanosheets to N-doped carbon nanotubes to promote enhanced performance of a zinc–air battery. Chemical Communications, 2020, 56, 8277-8280.	4.1	15
25	Long Carrier Diffusion Length and Slow Hot Carrier Cooling in Thin Film Mixed Halide Perovskite. IEEE Journal of Photovoltaics, 2020, 10, 803-810.	2.5	16
26	An earth-abundant bimetallic catalyst coated metallic nanowire grown electrode with platinum-like pH-universal hydrogen evolution activity at high current density. Chemical Science, 2020, 11, 3893-3902.	7.4	42
27	Charge Transfer and Ultrafast Nonlinear Optical Properties above Percolation Threshold in Graphene-Induced ZnTTBPc. Journal of Physical Chemistry C, 2020, 124, 7039-7047.	3.1	2
28	When multiferroics become photoelectrochemical catalysts: A case study with BiFeO3/La2NiMnO6. Materials Chemistry and Physics, 2020, 244, 122685.	4.0	10
29	All-inorganic quantum dot assisted enhanced charge extraction across the interfaces of bulk organo-halide perovskites for efficient and stable pin-hole free perovskite solar cells. Chemical Science, 2019, 10, 9530-9541.	7.4	43
30	Attuning the Electronic Properties of Two-Dimensional Co-Fe-O for Accelerating Water Electrolysis and Photolysis. ACS Applied Materials & amp; Interfaces, 2019, 11, 30682-30693.	8.0	16
31	Bimetallic nanoparticle decorated perovskite oxide for state-of-the-art trifunctional electrocatalysis. Journal of Materials Chemistry A, 2019, 7, 19453-19464.	10.3	68
32	Surface Charge Modulation of Perovskite Oxides at the Crystalline Junction with Layered Double Hydroxide for a Durable Rechargeable Zinc–Air Battery. ACS Applied Materials & Interfaces, 2019, 11, 35853-35862.	8.0	40
33	Limiting Heterovalent B-Site Doping in CsPbl ₃ Nanocrystals: Phase and Optical Stability. ACS Energy Letters, 2019, 4, 1364-1369.	17.4	86
34	The destructive spontaneous ingression of tunable silica nanosheets through cancer cell membranes. Chemical Science, 2019, 10, 6184-6192.	7.4	6
35	Photocatalyzed borylation using water-soluble quantum dots. Chemical Communications, 2019, 55, 6201-6204.	4.1	38
36	Doping the Smallest Shannon Radii Transition Metal Ion Ni(II) for Stabilizing α-CsPbI ₃ Perovskite Nanocrystals. Journal of Physical Chemistry Letters, 2019, 10, 7916-7921.	4.6	53

#	Article	IF	CITATIONS
37	Cation Exchange in Zn–Ag–In–Se Core/Alloyed Shell Quantum Dots and Their Applications in Photovoltaics and Water Photolysis. Chemistry of Materials, 2019, 31, 161-170.	6.7	15
38	Interface Engineering in Quantum-Dot-Sensitized Solar Cells. Langmuir, 2018, 34, 10197-10216.	3.5	34
39	Molybdenum sulfide–reduced graphene oxide p–n heterojunction nanosheets with anchored oxygen generating manganese dioxide nanoparticles for enhanced photodynamic therapy. Chemical Science, 2018, 9, 8982-8989.	7.4	40
40	High performance duckweed-derived carbon support to anchor NiFe electrocatalysts for efficient solar energy driven water splitting. Journal of Materials Chemistry A, 2018, 6, 18948-18959.	10.3	58
41	Cobalt Phosphide Nanorods with Controlled Aspect Ratios as Synergistic Photothermo-Chemotherapeutic Agents. ACS Applied Nano Materials, 2018, 1, 5237-5245.	5.0	13
42	Value added transformation of ubiquitous substrates into highly efficient and flexible electrodes for water splitting. Nature Communications, 2018, 9, 2014.	12.8	126
43	Maneuvering the Physical Properties and Spin States To Enhance the Activity of La–Sr–Co–Fe–O Perovskite Oxide Nanoparticles in Electrochemical Water Oxidation. ACS Applied Energy Materials, 2018, 1, 3342-3350.	5.1	29
44	Dependence of halide composition on the stability of highly efficient all-inorganic cesium lead halide perovskite quantum dot solar cells. Solar Energy Materials and Solar Cells, 2018, 185, 28-35.	6.2	82
45	Photoactive Core–Shell Nanorods as Bifunctional Electrodes for Boosting the Performance of Quantum Dot Sensitized Solar Cells and Photoelectrochemical Cells. Chemistry of Materials, 2018, 30, 6071-6081.	6.7	39
46	Chemical Modifications of Porous Carbon Nanospheres Obtained from Ubiquitous Precursors for Targeted Drug Delivery and Live Cell Imaging. ACS Sustainable Chemistry and Engineering, 2018, 6, 8503-8514.	6.7	22
47	Zinc-diffused silver indium selenide quantum dot sensitized solar cells with enhanced photoconversion efficiency. Journal of Materials Chemistry A, 2017, 5, 11746-11755.	10.3	43
48	Enhancing Multifunctionality through Secondary Phase Inclusion by Self-Assembly of Mn ₃ O ₄ Nanostructures with Superior Exchange Anisotropy and Oxygen Evolution Activity. Journal of Physical Chemistry C, 2017, 121, 25594-25602.	3.1	19
49	Coexistence of High Magnetization and Anisotropy with Non-monotonic Particle Size Effect in Ferromagnetic PrMnO ₃ Nanoparticles. Journal of Physical Chemistry C, 2017, 121, 21029-21036.	3.1	10
50	Porous NiFe-Oxide Nanocubes as Bifunctional Electrocatalysts for Efficient Water-Splitting. ACS Applied Materials & Interfaces, 2017, 9, 41906-41915.	8.0	229
51	Lead free double perovskite oxides Ln 2 NiMnO 6 (Ln = La, Eu, Dy, Lu), a new promising material for photovoltaic application. Materials Science and Engineering B: Solid-State Materials for Advanced Technology, 2017, 226, 10-17.	3.5	82
52	Surfactant-Mediated Resistance to Surface Oxidation in MnO Nanostructures. ACS Omega, 2017, 2, 3028-3035.	3.5	9
53	Phenomenal Ultraviolet Photoresponsivity and Detectivity of Graphene Dots Immobilized on Zinc Oxide Nanorods. ACS Applied Materials & Interfaces, 2016, 8, 35496-35504.	8.0	60
54	A microwave synthesized Cu _x S and graphene oxide nanoribbon composite as a highly efficient counter electrode for quantum dot sensitized solar cells. Nanoscale, 2016, 8, 10632-10641.	5.6	54

#	Article	IF	CITATIONS
55	Extensive Parallelism between Crystal Parameters and Magnetic Phase Transitions of Unusually Ferromagnetic Praseodymium Manganite Nanoparticles. Inorganic Chemistry, 2016, 55, 7903-7911.	4.0	4
56	Carbon dots with tunable concentrations of trapped anti-oxidant as an efficient metal-free catalyst for electrochemical water oxidation. Journal of Materials Chemistry A, 2016, 4, 14614-14624.	10.3	39
57	Efficient Dye Degradation Catalyzed by Manganese Oxide Nanoparticles and the Role of Cation Valence. ChemistrySelect, 2016, 1, 4265-4273.	1.5	37
58	Influence of the morphology of carbon nanostructures on the stimulated growth of gram plant. RSC Advances, 2016, 6, 43864-43873.	3.6	24
59	High Pressure Experimental Studies on CuO: Indication of Re-entrant Multiferroicity at Room Temperature. Scientific Reports, 2016, 6, 31610.	3.3	30
60	Graphitic porous carbon derived from human hair as â€~green' counter electrode in quantum dot sensitized solar cells. Carbon, 2016, 107, 395-404.	10.3	60
61	Enhancement of Magnetization through Interface Exchange Interactions of Confined NiO Nanoparticles within the Mesopores of CoFe ₂ O ₄ . Journal of Physical Chemistry C, 2016, 120, 5523-5533.	3.1	23
62	Lemon grass derived porous carbon nanospheres functionalized for controlled and targeted drug delivery. Carbon, 2016, 100, 223-235.	10.3	45
63	Dual Sensitization Strategy for High-Performance Core/Shell/ <i>Quasi-shell</i> Quantum Dot Solar Cells. Chemistry of Materials, 2015, 27, 4848-4859.	6.7	56
64	Plight of Mn Doping in Colloidal CdS Quantum Dots To Boost the Efficiency of Solar Cells. Journal of Physical Chemistry C, 2015, 119, 13404-13412.	3.1	42
65	A Fragmentizing Interface to a Large Corpus of Digitized Text: (Post)humanism and Non-consumptive Reading via Features. Interdisciplinary Science Reviews, 2015, 40, 61-77.	1.4	3
66	Iron Nitride Family at Reduced Dimensions: A Review of Their Synthesis Protocols and Structural and Magnetic Properties. Journal of Physical Chemistry C, 2015, 119, 1601-1622.	3.1	110
67	Enhanced catalytic activity of palladium nanoparticles confined inside porous carbon in methanol electro-oxidation. Green Chemistry, 2015, 17, 1572-1580.	9.0	31
68	Advanced Nanoporous Materials: Synthesis, Properties, and Applications. Journal of Nanomaterials, 2014, 2014, 1-2.	2.7	8
69	Pd nanoparticle concentration dependent self-assembly of Pd@SiO2 nanoparticles into leaching resistant microcubes. Chemical Communications, 2014, 50, 10510-10512.	4.1	11
70	Enhanced Low-Field Magnetoresistance in La _{0.71} Sr _{0.29} MnO ₃ Nanoparticles Synthesized by the Nonaqueous Sol–Gel Route. Chemistry of Materials, 2014, 26, 1702-1710.	6.7	70
71	Direct Correlation of the Morphologies of Metal Carbonates, Oxycarbonates, and Oxides Synthesized by Dry Autoclaving to the Intrinsic Properties of the Metals. Crystal Growth and Design, 2014, 14, 4060-4067.	3.0	5
72	One-Step Synthesis, Structural and Optical Characterization of Self-Assembled ZnO Nanoparticle Clusters with Quench-Induced Defects. Science of Advanced Materials, 2014, 6, 1160-1169.	0.7	29

SAYAN BHATTACHARYYA

#	Article	IF	CITATIONS
73	Single-step scalable conversion of waste natural oils to carbon nanowhiskers and their interaction with mammalian cells. Journal of Nanoparticle Research, 2013, 15, 1.	1.9	11
74	Analysis of the acid, base and air oxidized carbon microspheres synthesized in a single step from waste engine oil. Corrosion Science, 2013, 73, 356-364.	6.6	12
75	Stacked Nanosheets of Pr1–xCaxMnO3 (x = 0.3 and 0.49): A Ferromagnetic Two-Dimensional Material with Spontaneous Exchange Bias. Journal of Physical Chemistry C, 2013, 117, 26351-26360.	3.1	19
76	Ferromagnetism in Lightly Doped Pr _{1–<i>x</i>} Ca _{<i>x</i>} MnO ₃ (<i>x</i> = 0.023, 0.036) Nanoparticles Synthesized by Microwave Irradiation. Chemistry of Materials, 2012, 24, 3758-3764.	6.7	16
77	Magnetic properties of Cd _{1 â^'<i>x</i>} Mn _{<i>x</i>} Te/C nanocrystals. Nanotechnology, 2011, 22, 075703.	2.6	6
78	Ab Initio Study of the Structural, Electronic, Magnetic, and Hyperfine Properties of Ga _{<i>x</i>} Fe _{4–<i>x</i>} N (0.00 ≤i>x ≤.00) Nitrides. Journal of Physical Chemistry C, 2011, 115, 23081-23089.	3.1	11
79	Optical and Structural Studies of Phase Separation in Zn[sub x]Cd[sub 1â^'x]Seâ^•C Coreâ^•Shell Nanocrystals. , 2011, , .		1
80	Multifunctional carbon-nanotube cellular endoscopes. Nature Nanotechnology, 2011, 6, 57-64.	31.5	214
81	Electron Paramagnetic Resonance Spectroscopic Investigation of Manganese Doping in ZnL (L = O, S,) Tj ETQq1	1 0.78431 0.4	4 rgBT /Over
82	Synthesis and magnetic characterization of CoMoN2 nanoparticles. Journal of Nanoparticle Research, 2010, 12, 1107-1116.	1.9	13
83	Copper Azide Confined Inside Templated Carbon Nanotubes. Advanced Functional Materials, 2010, 20, 3168-3174.	14.9	73
84	Variation of magnetic ordering in ε-Fe3N nanoparticles. Chemical Physics Letters, 2010, 496, 122-127.	2.6	22
85	Phase-separation in ZnxCd1-xSe/C Core/shell nanocrystals studied with cathodoluminescence spectroscopy. Materials Research Society Symposia Proceedings, 2010, 1260, 1.	0.1	0
86	Luminescent and Ferromagnetic CdS:Mn ²⁺ /C Coreâ^'Shell Nanocrystals. Journal of Physical Chemistry C, 2010, 114, 22002-22011.	3.1	32
87	Investigation of γ′-Fe4Nâ^'GaN Nanocomposites: Structural and Magnetic Characterization, Mössbauer Spectroscopy and Ab Initio Calculations. Journal of Physical Chemistry C, 2010, 114, 17542-17549.	3.1	8
88	Small diameter carbon nanopipettes. Nanotechnology, 2010, 21, 015304.	2.6	69
89	Carrier relaxation dynamics of ZnxCd1â^'xSe/C core/shell nanocrystals with phase separation as studied by time-resolved cathodoluminescence. Applied Physics Letters, 2009, 95, 181903.	3.3	2
90	Localized Synthesis of Metal Nanoparticles Using Nanoscale Corona Discharge in Aqueous Solutions. Advanced Materials, 2009, 21, 4039-4044.	21.0	29

#	Article	IF	CITATIONS
91	A One-step, Template-free Synthesis, Characterization, Optical and Magnetic Properties of Zn _{1â^²<i>x</i>} Mn _{<i>x</i>} Te Nanosheets. Chemistry of Materials, 2009, 21, 326-335.	6.7	37
92	Highly Luminescent ZnxCd1â^'xSe/C Core/Shell Nanocrystals: Large Scale Synthesis, Structural and Cathodoluminescence Studies. ACS Nano, 2009, 3, 1864-1876.	14.6	24
93	Observation of exchange bias and spin-glass-like ordering in É›-Fe2.8Cr0.2N nanoparticles. Pramana - Journal of Physics, 2008, 70, 367-373.	1.8	9
94	One‣tep Solventâ€Free Synthesis and Characterization of Zn _{1â^'x} Mn _x Se@C Nanorods and Nanowires. Advanced Functional Materials, 2008, 18, 1641-1653.	14.9	31
95	A template-free, sonochemical route to porous ZnO nano-disks. Microporous and Mesoporous Materials, 2008, 110, 553-559.	4.4	113
96	Microwave-Assisted Insertion of Silver Nanoparticles into 3-D Mesoporous Zinc Oxide Nanocomposites and Nanorods. Journal of Physical Chemistry C, 2008, 112, 659-665.	3.1	89
97	Spin-glass-like ordering in É›-Fe3â˜xNixN (0.1â‰ ¤ â‰ θ .8) nanoparticles. Materials Chemistry and Physics, 2008, 108, 201-207.	4.0	21
98	Synthesis and characterization of É›-Fe3N/GaN, 54/46-composite nanowires. Materials Research Bulletin, 2008, 43, 272-283.	5.2	15
99	Synthesis, Characterization, and Room-Temperature Ferromagnetism in Cobalt-Doped Zinc Oxide (ZnO:Co ²⁺) Nanocrystals Encapsulated in Carbon. Journal of Physical Chemistry C, 2008, 112, 4517-4523.	3.1	30
100	Interplay of Porosity in γ-Al ₂ O ₃ -Doped ZnO Nanocomposites: A Comparative Study of Sonochemical and Microwave Reaction Routes. Journal of Physical Chemistry C, 2008, 112, 13156-13162.	3.1	13
101	One-Pot Synthesis and Characterization of Mn2+-Doped Wurtzite CdSe Nanocrystals Encapsulated with Carbon. Journal of Physical Chemistry C, 2008, 112, 7624-7630.	3.1	27
102	One-pot fabrication and magnetic studies of Mn-doped TiO ₂ nanocrystals with an encapsulating carbon layer. Nanotechnology, 2008, 19, 495711.	2.6	35
103	Exchange Bias and Spin-Glass-Like Ordering inε-Fe3N–CrN Nanocomposites. Japanese Journal of Applied Physics, 2007, 46, 980-987.	1.5	10
104	Magnetic interactions in ε-Fe3N–GaN nanocomposites. Journal of Applied Physics, 2007, 101, 113902.	2.5	13
105	Synthesis, Characterization and Magnetic Interactions Study of ε-Fe3N–CrN Nanorods. Journal of Nanoscience and Nanotechnology, 2007, 7, 1836-1840.	0.9	10
106	Mössbauer and magnetic studies of MFe2O4(M = Co, Ni) nanoparticles. Hyperfine Interactions, 2007, 1 153-159.	165 0.5	33
107	Sonochemical Insertion of Silver Nanoparticles into Two-Dimensional Mesoporous Alumina. Journal of Physical Chemistry C, 2007, 111, 11161-11167.	3.1	32
108	Mössbauer studies of É›-Fe3â^'x Ni x N and γ′-Fe4â^'y Ni y N nanoparticles. Hyperfine Interactions, 2007, 165, 147-151.	0.5	7

#	Article	IF	CITATIONS
109	Synthesis and structural investigation of É›-Fe3â^'xNixN (0.0â‰ ¤ â‰ 9 .8) nanoparticles. Progress in Crystal Growth and Characterization of Materials, 2006, 52, 132-141.	4.0	9
110	Magnetic Properties of Co and Ni Substituted É›-Fe3N Nanoparticles. Hyperfine Interactions, 2006, 164, 17-26.	0.5	22
111	Magnetic properties of ε-Fe3N–GaN core–shell nanowires. Nanotechnology, 2005, 16, 2012-2019.	2.6	28
112	Mössbauer Studies of Nanosize CuFe2O4Particles. Hyperfine Interactions, 2004, 156/157, 57-61.	0.5	26
113	Magnetism of nanostructured iron nitride (Fe-N) systems. Physica Status Solidi C: Current Topics in Solid State Physics, 2004, 1, 3252-3259.	0.8	14
114	Magnetic properties ofÉ›-Fe3-xNixN nanoparticles. Physica Status Solidi C: Current Topics in Solid State Physics, 2004, 1, 3764-3768.	0.8	7